Hydrodynamic Interaction between a Spherical Particle and an Elastic Surface: A Gentle Probe for Soft Thin Films

Samuel Leroy,[1] Audrey Steinberger,[1] Cécile Cottin-Bizonne,[1] Frédéric Restagno,[2] Liliane Léger,[2] and Élisabeth Charlaix[1]
[1]Université Lyon 1-Université de Lyon-CNRS, Laboratoire PMCN, F-69622 Villeurbanne, France
[2]Laboratoire de Physique des Solides, Université Paris-Sud-CNRS, F-91405 Orsay, France
(Received 24 November 2011; published 26 June 2012)

We study the hydrodynamic interaction between a sphere and an elastic surface at a nanoscale with a dynamic surface force apparatus. We show that the interplay between viscous forces and elastic deformations leads to very rich scaling properties of the force response, providing a unique signature of the surface elastic behavior. These properties are illustrated on three different examples: a thick elastomer, a thin elastomer film, and a layer of micrometric bubbles. We show that this fluid probing allows one to measure the Young's modulus of surfaces and soft thin layers at distance, without any direct solid-solid contact.

DOI: 10.1103/PhysRevLett.108.264501 PACS numbers: 47.15.G−, 68.08.−p, 68.60.−p

The nano-mechanics of soft, thin materials, such as polymer coatings, has become an important issue with the development of composite and nano-composite new materials and their applications in many industrial processes (surface coatings, stability of structures used in microelectronics, etc.) [1–4]. Direct characterization based on touching the surface with a solid probe does not always provide an absolute determination of elastic moduli, since adhesion and friction forces are intrinsically of the same magnitude as the elastic forces [5–7]. In some extreme cases, such as bubbles or biological systems, contact forces can even ruin the sample. A naive idea would be to blow gently on these soft surfaces to deform them without touching them. In this Letter, we rather demonstrate that a liquid probe can be an alternative to classical hard contact mechanics. More precisely, we show that the nano-hydrodynamic interaction between a sphere and a soft layer supported on a rigid substrate can provide a new, precise, and faithful method for measuring its absolute elastic properties. Indeed in the past ten years, surface forces measurements and more generally very weak forces measurements have reached an encompassed precision [8–11] and nano-hydrodynamic forces have been used to probe the friction at a solid-liquid interface. We extend here the use of nanoflows to measure the mechanical properties of surfaces.

We use the nanoscale flow created by a sphere which is oscillated at a very small amplitude in the direction normal to the tested surface. We use to create this flow a surface force apparatus (SFA) [12]. The fluid layer between the sphere and the plane is forced to drain inward and outward of the gap, generating a dynamic pressure at the excitation frequency $\omega/2\pi$. More specifically, we define the dynamic response $\tilde{G}_\omega(D) = \tilde{F}_\omega/h_0$ as the ratio of the complex amplitude $\tilde{F}_\omega$ of the hydrodynamicforce to the amplitude h_0 of the oscillating motion [Fig. 1(a)]. If the probed surface is perfectly rigid, the force applied by the flow is the so-called Reynolds force of amplitude $\mathcal{R}(D) = 6\pi\eta h_0 \omega R^2/D$, η being the fluid viscosity and D the sphere—surface distance. An important feature of the Reynolds flow is that the radial extension of the applied pressure is of order $\sqrt{2RD}$. Thus, when the distance is varied, the hydrodynamic force and the probed area vary in opposite ways, resulting in a great flexibility of this mechanical essay. If the target surface is not rigid but elastically compliant, the lubrication flow couples to its elastic deformation. In a recent paper, we have calculated theoretically the elasto-hydrodynamic (EHD) linear response $\tilde{G}_\omega(D)$ as a function of the Young's modulus E and the Poisson ration ν of the material [13]. In this Letter, we demonstrate that the precise measurement of $\tilde{G}_\omega(D)$ allows for an absolute determination of the elastic modulus of the surface without further assumption on adhesion properties. This experimental proof is performed on three examples which illustrate the three possible types of elasto-hydrodynamic interactions.

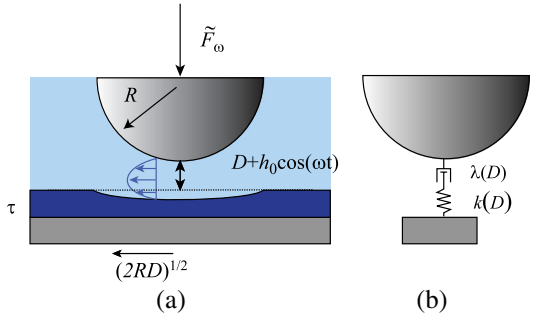

FIG. 1 (color online). Principle of the experiment. (a) A surface force apparatus creates a flow between a sphere and an elastic film (the sphere oscillates with an amplitude h_0 at a frequency $f = \omega/2\pi$). The typical distance over which the flow probes the soft surface quotes $\sqrt{2RD}$. (b) Spring-and-dashpot model equivalent to the system. The dashpot characteristic is given by the Reynolds force.

As a first example we study a thick (1 mm) elastomer made of reticulated polydimethylsiloxane (PDMS; SYLGARD 184, Dow Corning), cured at 50 °C for 24 h. A water—glycerol solution of viscosity $\eta = 12$ mPa · s is the fluid probe. The dynamic force response plotted as a function of D in Fig. 2 shows two regimes. At large distance, the response is dominated by the reference viscous damping $G''_\omega = 6\pi\eta\omega R^2/D$. The compliance of the elastomer appears through the small real part $G'_\omega(D)$ scaling as $1/D^{5/2}$. This is the viscous regime. As the distance decreases, the two components G'_ω and G''_ω become eventually of same magnitude and saturate at a constant value. In this elastic regime, the damping does not diverge as $1/D$ because the fluid is no longer expelled from the gap between the surfaces. The elastic surface does not sustain the viscous pressure and accommodates for most of the sphere displacement h_0.

It is of interest to describe this scaling with a semiquantitative model. At large distance, the hydrodynamic force is weak and does not indent the elastomer significantly. The fluid probe acts as a dashpot of damping coefficient $\lambda(D) = 6\pi\eta R^2/D$ applying a pressure $\mathcal{R}(D)/2\pi RD$ over the area $2\pi RD$. The target surface responds to this localized stress as a semi-infinite medium, with a stiffness $k(D) = E^*\pi\sqrt{2RD}$ [14]. Here, $E^* = E/(1-\nu^2)$ is the reduced Young's modulus of the elastomer. The nondimensional number $\lambda\omega/k = (D_k/D)^{3/2}$ defines a crossover length $D_k = 8R(\eta\omega/E^*)^{2/3}$. The amplitude of the surface indentation is $\delta = \mathcal{R}/k \simeq h_0(D_k/D)^{3/2}$. Thus, the small indentation limit corresponds to the viscous regime observed for $D \gg D_k$. The force response of this spring-and-dashpot in series, $G_\omega = (1/k + 1/i\lambda\omega)^{-1}$, can be expanded as $G_\omega \sim i\lambda\omega + (\lambda\omega)^2/k$. One recovers a real part G'_ω scaling as $D^{-5/2}$. When D becomes lower than D_k, the flow separates in two regions. In a central region where the liquid thickness is lower than D_k, the liquid clamped by its viscosity acts as a solid probe. The elastic indentation of the target surface accommodates fully for the sphere oscillation. Outside this region, the features of the Reynolds flow are recovered. The system is now a spring-and-dashpot in parallel, and the response saturates to $G_\omega \sim k(D_k) + i\omega\lambda(D_k)$, more or less close to its crossover value. Thus, this simple model accounts semiquantitatively for the experimental results. In the full theoretical analysis, we have shown that the EHD response of a bulk medium is fully described by the single parameter D_k via a master function g_k tabulated in [13]:

$$G_\omega(D) = \frac{6\pi\eta\omega R^2}{D_k} g_k\left(\frac{D}{D_k}\right), \tag{1}$$

with $g_k(0) = 2.015 + 1.163i$ and $g_k(x \gg 1) = i/x + 0.173/x^{5/2}$. This master function reproduces well the scaling of the data, shown in Fig. 2(a) for the forcing frequency $\omega/2\pi = 19$ Hz. By fitting the $D^{-5/2}$ decay of the real part we obtain an estimate of the critical distance $D_k \sim 1.25\,\mu$m. This gives the minimum value of the hydrodynamic radius $\sqrt{2RD_k} = 100\ \mu$m. This value is not very small compared to the film thickness, leading to finite size effect which is clear in Fig. 2(a). Using the full theory which takes into account the finite film thickness [13], we obtain an excellent agreement as well as the refined value $D_k = 1.455\ \mu$m. The same procedure for an experiment performed at a forcing frequency of 39 Hz gives $D_k(39\text{ Hz}) = 2.455\ \mu$m [see Fig. 2(b)]. The ratio $D_k(19\text{ Hz})/D_k(39\text{ Hz}) = 0.593$ is very close to the frequency ratio $(19/39)^{2/3} = 0.619$ predicted by our analysis. The relative difference of 4% shows the accuracy of our technique. Taking a Poisson ratio $\nu = 1/2$, we derive a value of the Young's modulus $E = 2.7 \pm 0.1$ MPa for this reticulated PDMS.

The case of a bulk medium illustrated above is obtained when the thickness τ of the elastic layer is much larger than the fluid probe radius $\sqrt{2RD}$. An interesting second example is the thin film limit $\tau \ll \sqrt{2RD}$. Figure 3 shows a

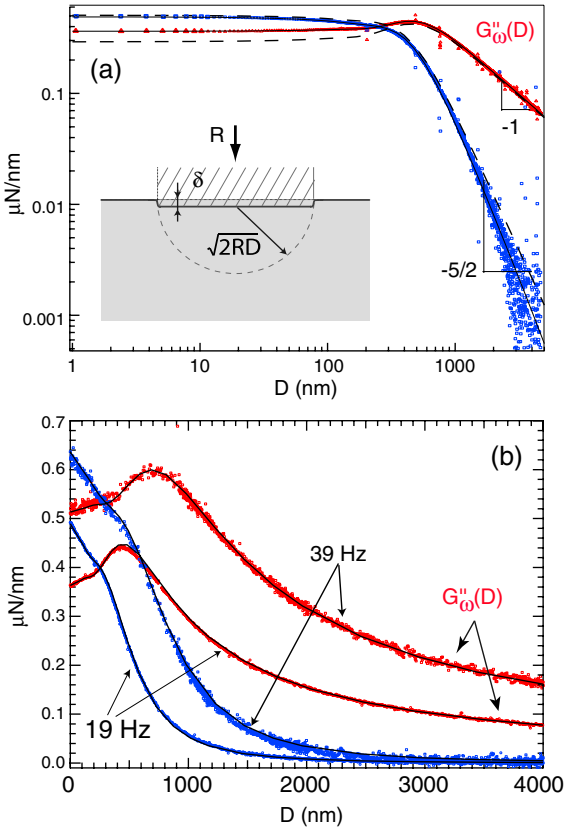

FIG. 2 (color online). Real part (blue) and imaginary part (red) of the force response $G_\omega(D)$ obtained on a reticulated PDMS of thickness 1 mm. (a) Log scale, $f = 19$ Hz; (b) linear scale, $f = 19$ Hz and $f = 39$ Hz. The sphere radius is 3.4 mm and the liquid viscosity is 12 ± 2 mPa · s. In (a) the dashed line plots $6\pi\eta\omega R^2 g_k/D_k$ as a function of D/D_k [Eq. (1)]. In (a) and (b) the continuous black line is the best fit of the linear EHD theory [13] with $D_k(19\text{ Hz}) = 1.455\ \mu$m and $D_k(39\text{ Hz}) = 2.455\ \mu$m. The inset represents a flat punch of radius $\sqrt{2RD}$ indenting a semi-infinite medium.

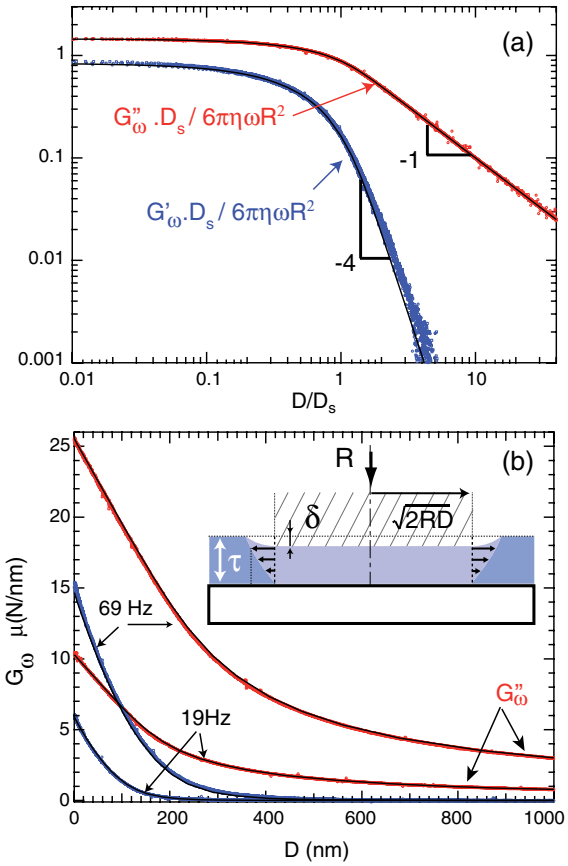

FIG. 3 (color online). (a) The scaled force response $G_\omega(D)D_s/6\pi\eta\omega R^2$ measured on a PDMS film of thickness 4.4 μm at two frequencies: $f = 69$ Hz (with $D_s = 170$ nm) and $f = 19$ Hz (with $D_s = 109$ nm). Blue: real part, red: imaginary part. The sphere radius is 3 mm and the liquid viscosity is 43 ± 2 mPa · s. The black continuous line is the master function g_s. (b) The force response $G_\omega(D)$ as a function of D in linear scale for the two frequencies. The continuous black lines are plots of the scaled master function g_s [right-hand side (rhs) of Eq. (2)].

4.4 μm reticulated PDMS film studied with the SFA ($R = 3$ mm) using a glycerolwater mixture of viscosity 43 ± 2 mPa · s. The thin film was deposited on a floated Pyrex plane by spin coating a solution of PDMS (30% in heptane) mixed with the curing agent (SYLGARD, Dow Corning, reticulating ratio 10:1). After deposition the samples were cured first at 150 °C for 1 h, and then at 75 °C over a night in an oven.

As previously the force response shows a viscous regime at large distance and saturates at small distance. However, the response is much stiffer than the one of the thick layer: the real part G'_ω is always lower than the dissipative part G''_ω, and decays as $1/D^4$ in the viscous regime. This stiff behavior of the incompressible elastomer is due to its confinement: the layer has to expand in its own plane in order to compensate for an indentation in the transverse direction. This enhanced stiffness due to confinement has been described in the domain of contact mechanics, such as the so-called Johnson-Kendall-Roberts tests [7,15]. It leads to an elastic pileup mechanism which prevents accurate measurements of moduli in the range of the MPa for layers whose thickness is less than the micrometer [16,17]. In the case of the fluid probe, the in-plane displacement u_r of the layer at the border of the stressed area compensating an indentation δ is $u_r = RD\delta/\tau\sqrt{2RD}$. As the layer is clamped on the underlying Pyrex substrate, this displacement induces a shear of order $\epsilon \sim u_r/\tau$. The stored elastic energy $\mathcal{R}\delta \sim (\mu\epsilon^2/2)2\pi RD\tau$, with $\mu = E/3$ the shear modulus of the elastomer, determines the stiffness of the confined layer $k(D) = \mathcal{R}/\delta \sim 4\pi R^2D^2E/3\tau^3$. Note that this stiffness depends more severely on the sphere-plane distance than the one of the thick layers, which scaled as $\sqrt{D}$. This gives a new cutoff distance $D_s = \tau(4\eta\omega/E)^{1/3}$ defined from $\lambda\omega/k = (D_s/D)^3$. The cutoff distance of the confined layer is proportional to its thickness and depends only as the one-third power of its modulus. The real part of the force response in the viscous regime $G'_\omega \sim (\lambda\omega)^2/k$ vanishes as $1/D^4$.

The theoretical EHD response of the confined incompressible layer writes [3]:

$$D_s = \tau\left(\frac{4\eta\omega}{E}\right)^{1/3} G_\omega(D) = \frac{6\pi\eta\omega R^2}{D_s} g_s\left(\frac{D}{D_s}\right),$$
$$g_s(0) = 0.838(1 + i\sqrt{3}) \lim_{x\to\infty} g_s(x) = \frac{3}{10x^4} + \frac{i}{x} \qquad (2)$$

with the intermediate values of g_s tabulated in [13]. As in the thick film case, the agreement with the data obtained by fitting the single parameter D_s is excellent. In particular, our model predicts $G'(0)/G''(0) = 1/\sqrt{3}$ as observed. More precisely we find cutoff values $D_s(19\text{ Hz}) = 109 \pm 1$ nm and $D_s(69\text{ Hz}) = 170 \pm 1$ nm. Their ratio equals to 0.647, which is very close to the theoretical ratio $(19/69)^{1/3} = 0.651$. The derived value of the Young's modulus is $E = 1.3 \pm 0.1$ MPa. It is important to mention that the main uncertainty in the value of E comes from the value of the film thickness $\tau = 4.4 \pm 0.1$ μm.

A third example is the case of individual, compressible objects resting on a rigid surface, such as bubbles. We illustrate this case with an array of microbubbles embedded in the holes of a textured, hydrophobic surface (Fig. 4). The fluid probe is a water-glycerol mixture of viscosity $\eta = 39 \pm 2$ mPa · s. In a previous study, we showed that running nanorheology experiments with the dynamic SFA on such a soft surface allowed us to measure the surface stiffness of the bubble mattress, defined as κn with κ the stiffness of a single bubble and n the number of bubble per unit surface [18]. We want to stress here that this configuration is formally equivalent to a compressible layer of thickness τ and uniaxial compression modulus $E' = E(1-\nu)/(1-2\nu)(1+\nu) = \kappa n\tau$. When the viscous stress $\mathcal{R}/2\pi RD$ is applied by the fluid probe, the compressible layer indents as $\delta = \tau\mathcal{R}/2\pi RDE'$, and its

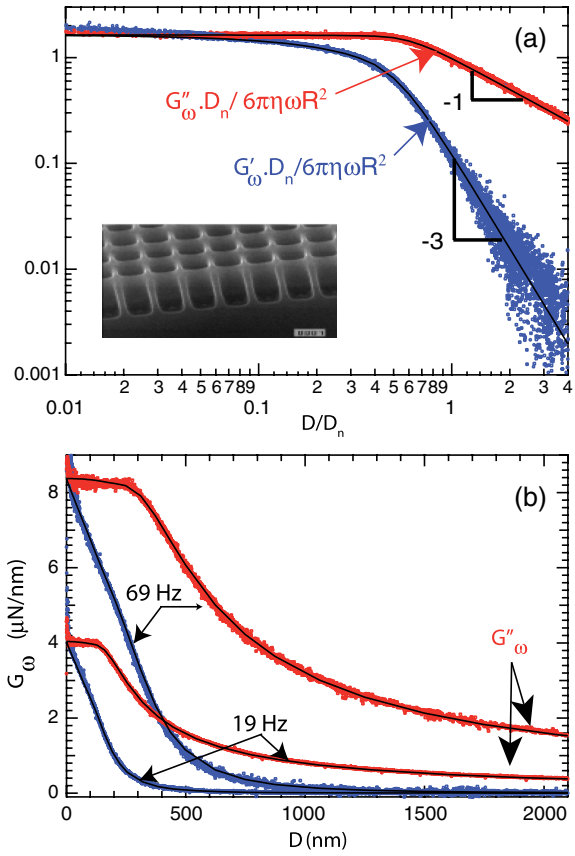

FIG. 4 (color online). (a) The scaled force response $G_\omega(D)D_n/6\pi\eta\omega R^2$ measured on a regular array of submicrometric bubbles embedded in the holes of a textured silanized silicon surface. Red: imaginary part, blue: real part. Two frequencies are overlayed: $f = 69$ Hz (with $D_n = 320$ nm) and $f = 19$ Hz (with $D_n = 624$ nm). The black lines are the components of the master function g_n [Eq. (3)]. (b) The force response $G_\omega(D)$ as a function of D in linear scale. The black lines are plots of the rhs of Eq. (3).

effective stiffness for the spring-and-dashpot model is $k(D) = 2\pi RDE'/\tau$. The associated cutoff length is $D_n = \sqrt{2\eta\omega R\tau/E'}$ and the real part decays as $(\omega\lambda)^2/k \sim 1/D^3$ in the viscous regime as observed in Fig. 4. The theoretical EHD response has the form:

$$D_n = \left(\frac{2\eta\omega R\tau}{E'}\right)^{1/2} G_\omega(D) = \frac{6\pi\eta\omega R^2}{D_n} g_n\left(\frac{D}{D_n}\right),$$
$$g_n(0) = \sqrt{2/3}(1+i) \lim_{x\to\infty} g_n(x) = \frac{1}{2x^3} + \frac{i}{x} \qquad (3)$$

with the master function g_n tabulated in [13]. Once again, the agreement with the experimental data is excellent. The values found for D_n at 19 and 69 Hz, respectively 160 and 312 nm, are consistent with the same value of the mattress stiffness $\kappa n = E'/\tau = 1.1 \pm 0.1 \times 10^{12}$ N · m as obtained in [18]. This is expected at frequencies much lower than the resonance frequency of the microbubbles [19]. Our model also predicts, as observed, that $G'(0)/G''(0) = 1$. This example demonstrates the nonintrusive character of the fluid probe method, as any contact of a solid probe with the bubbles would change their shape and alter their stiffness.

In conclusion, we demonstrate here with a SFA that hydrodynamic interactions at a nanoscale provide a unique tool for the quantitative testing of small and soft elastic objects, allowing one to measure unambiguously their elastic properties without contact. The interplay between viscous and elastic effects results in a very rich scaling of the force response and provides a signature of the surface elastic behavior without the influence of adhesion forces. We have chosen here to illustrate three different cases: thick layer, thin compressible, and thin incompressible film, which obey three different master functions. The excellent agreement of the calculated scaling laws with the experimental data shows that the method is suitable for measuring a wide range of elastic moduli, depending only on the capabilities of the experimental device. For the best resolution, the fluid probe viscosity should be chosen such that the crossover distance lies in the range of the available experimental distances (typically 20 nm to 2 μm in our SFA). For instance, a bulk glass with Young's modulus $E = 60$ GPa probed at 100 Hz with a viscosity of 10^{-1} Pa · s corresponds to $D_c = 24$ nm, whereas a soft tissue of modulus 1 kPa probed at 15 Hz with air ($\eta = 2 \times 10^{-5}$ Pa · s) gives a crossover distance of 2.4 μm. A layer of 200 nm of the same material probed at 100 Hz with water would have a crossover distance of 27 nm. This method thus opens the route for a quantitative elastic imaging of soft surfaces. Using colloidal probe atomic force microscopy would increase the frequency range of this mechanical testing, allowing one to probe the frequency dependence and possibly the viscoelastic properties of soft thin films. For this, it is necessary to measure the actual amplitude of the cantilever displacement and not just its deflection.

We acknowledge the financial support of ANR program Merig. We thank Christophe Poulard and Erasmo Ovalle-Garcia for their help in the sample preparation. We benefited from the AXELERA program.

[1] G. Reiter and J. Forrest, Eur. Phys. J. E **8**, 101 (2002).
[2] C. Stafford, C. Harrison, K. Beers, A. Karim, E. Amis, M. Vanlandingham, H.-C. Kim, W. Volksen, R. Miller, and E. Simonyi, Nat. Mater. **3**, 545 (2004).
[3] J. M. Torres, C. M. Stafford, and B. D. Vogt, ACS Nano **3**, 2677 (2009).
[4] W. Allers, C. Hahn, M. Lohndorf, S. Lukas, S. Pan, U. D. Schwarz, and R. Wiesendanger, Nanotechnology **7**, 346 (1996).
[5] K. Shull, Mater. Sci. Eng. R **36**, 1 (2002).
[6] P. McGuiggan, J. Wallace, D. Smith, I. Sridhar, Z. Zheng, and K. Johnson, J. Phys. D: Appl. Phys. **40**, 5984 (2007).
[7] M. Deruelle, H. Hervet, G. Jandeau, and L. Leger, J. Adhes. Sci. Technol. **12**, 225 (1998).

[8] C. Cottin-Bizonne, B. Cross, A. Steinberger, and E. Charlaix, Phys. Rev. Lett. **94**, 056102 (2005).
[9] A. Maali and B. Bhushan, Phys. Rev. E **78**, 027302 (2008).
[10] A. Siria, A. Drezet, F. Marchi, F. Comin, S. Huant, and J. Chevrier, Phys. Rev. Lett. **102**, 254503 (2009).
[11] S. de Man, K. Heeck, R. J. Wijngaarden, and D. Iannuzzi, Phys. Rev. Lett. **103**, 040402 (2009).
[12] F. Restagno, J. Crassous, E. Charlaix, C. Cottin-Bizonne, and M. Monchanin, Rev. Sci. Instrum. **73**, 2292 (2002).
[13] S. Leroy and E. Charlaix, J. Fluid Mech. **674**, 389 (2011).
[14] K. Johnson, *Contact Mechanics* (Cambridge University Press, Cambridge, England, 1985), 13th ed.
[15] K. L. Johnson, K. Kendall, and A. D. Roberts, Proc. R. Soc. Lond. A **324**, 301 (1971).
[16] E. Barthel, A. Perriot, A. Chateauminois, and C. Frétigny, Philos. Mag. **86**, 5359 (2006).
[17] E. Barthel, J. Adhes. **83**, 729 (2007).
[18] A. Steinberger, C. C. Cottin-Bizonne, P. Kleimann, and E. Charlaix, Phys. Rev. Lett. **100**, 134501 (2008).
[19] H. Rathgen, K. Sugiyama, C.-D. Ohl, D. Lohse, and F. Mugele, Phys. Rev. Lett. **99**, 214501 (2007).